Published OnlineFirst March 24, 2009; DOI: 10.1158/0008-5472.CAN-08-4295

Research Article

Inhibition of NOTCH Signaling by Gamma Secretase Inhibitor Engages the RB Pathway and Elicits Cell Cycle Exit in T-Cell Acute Lymphoblastic Leukemia Cells

Sudhir S. Rao,[1] Jennifer O'Neil,[3] Cole D. Liberator,[1] James S. Hardwick,[4] Xudong Dai,[5] Theresa Zhang,[1] Edyta Tyminski,[1] Jing Yuan,[1] Nancy E. Kohl,[1] Victoria M. Richon,[1] Lex H.T. Van der Ploeg,[1] Pamela M. Carroll,[1] Giulio F. Draetta,[1] A. Thomas Look,[2,3] Peter R. Strack,[1] and Christopher G. Winter[1]

[1]Merck Research Laboratories; [2]Department of Pediatric Oncology, Dana-Farber Cancer Institute; [3]Division of Hematology, Children's Hospital Boston, Boston, Massachusetts; [4]Merck Research Laboratories, West Point, Pennsylvania; and [5]Rosetta Inpharmatics, LLC, Merck & Co., Inc., Seattle, Washington

Abstract

NOTCH signaling is deregulated in the majority of T-cell acute lymphoblastic leukemias (T-ALL) as a result of activating mutations in *NOTCH1*. Gamma secretase inhibitors (GSI) block proteolytic activation of NOTCH receptors and may provide a targeted therapy for T-ALL. We have investigated the mechanisms of GSI sensitivity across a panel of T-ALL cell lines, yielding an approach for patient stratification based on pathway activity and also providing a rational combination strategy for enhanced response to GSI. Whereas the *NOTCH1* mutation status does not serve as a predictor of GSI sensitivity, a gene expression signature of NOTCH pathway activity does correlate with response, and may be useful in the selection of patients more likely to respond to GSI. Furthermore, inhibition of the NOTCH pathway activity signature correlates with the induction of the cyclin-dependent kinase inhibitors CDKN2D ($p19^{INK4d}$) and CDKN1B ($p27^{Kip1}$), leading to derepression of RB and subsequent exit from the cell cycle. Consistent with this evidence of cell cycle exit, short-term exposure of GSI resulted in sustained molecular and phenotypic effects after withdrawal of the compound. Combination treatment with GSI and a small molecule inhibitor of CDK4 produced synergistic growth inhibition, providing evidence that GSI engagement of the CDK4/RB pathway is an important mechanism of GSI action and supports further investigation of this combination for improved efficacy in treating T-ALL. [Cancer Res 2009;69(7):3060–8]

Introduction

The NOTCH signaling pathway is an evolutionarily conserved regulator of cell fate, differentiation, and growth (1, 2). In the hematopoietic system, NOTCH functions at multiple binary decision points. During lymphopoiesis, NOTCH1 activity drives uncommitted progenitor cells toward a T-cell fate, rather than B-cell commitment (3). Deregulated NOTCH1 is oncogenic, promoting the development of T-cell acute lymphoblastic leukemia (T-ALL). Somatic activating mutations in *NOTCH1* are present in >50% of patients with T-ALL (4, 5). *NOTCH1* is also the target of a recurrent, albeit rare translocation (t7;9)(q34;q34.3), that results in the expression of constitutively active cytoplasmic fragments of the receptor (6, 7). Expression of the active cytoplasmic domain of NOTCH1 (NICD) in murine bone marrow cells is sufficient to induce T-cell leukemia with high penetrance in mice (8).

In mammals, NOTCH signaling is mediated by four NOTCH receptors (NOTCH1–4) and five ligands related to the invertebrate orthologues Delta, Serrate, and Lag-2. Physiologic NOTCH signaling is activated by a series of proteolytic cleavage events, culminating in the release of the intracellular domain (NICD) via ligand-dependent cleavage mediated by the gamma secretase (GS) complex. Upon GS cleavage, NICD translocates to the nucleus in which it binds to the transcription factor CSL and other proteins, and activates the transcription of NOTCH target genes. The best characterized NOTCH target genes are bHLH transcription factors of the hairy enhancer of split (HES) gene family, including *HES1, HES5, HEY1, HEY2*, and *HEYL* (3).

The prevalence of *NOTCH1* activating mutations in T-ALL patient samples suggests that NOTCH is a core oncogenic pathway in this disease and therefore a prime therapeutic target. Gamma secretase inhibitors (GSI) hold promise as targeted therapy for malignancies that are driven by aberrant NOTCH activity, such as T-ALL. Although the presence of activating mutations within *NOTCH1* suggests that the cells are dependent on the receptor, not all *NOTCH* mutated cell lines are sensitive to GSI (4). These results indicate that mutational status may not be an effective predictive marker for response to GSI in the clinic. A detailed understanding of the downstream signaling network that is engaged by NOTCH in T-ALL cells would shed light on such mechanisms, revealing markers that may help predict patients that would respond to GSIs. A better understanding of the NOTCH signaling pathway would also provide a rational basis for choosing therapeutics that could be combined with GSIs to improve therapeutic benefit. Recent studies have begun to reveal some of the pathways engaged by NOTCH in T-ALL cells. NOTCH directly induces *MYC* transcription and overexpression of *MYC* confers GSI resistance to T-ALL cells *in vitro* (9–11). The nuclear factor κB and mTOR pathways have recently been shown to be activated by NOTCH, providing a rationale for combination therapies with bortezomib and rapamycin analogues, respectively (12, 13).

Deregulation of cyclin D–dependent kinases (CDK4 and CDK6) and RB signaling is a common feature of T-ALL. CDKN2A ($p16^{INK4a}$), which imposes negative regulatory control on CDK4

Note: Supplementary data for this article are available at Cancer Research Online (http://cancerres.aacrjournals.org/).

S.S. Rao and J. O'Neil contributed equally to this work.

Requests for reprints: Christopher G. Winter, Merck Research Laboratories, 33 Avenue Louis Pasteur, Boston, MA 02115. Phone: 617-992-2290; Fax: 617-992-2411; E-mail: christopher_winter@merck.com.

doi:10.1158/0008-5472.CAN-08-4295

Published OnlineFirst March 24, 2009; DOI: 10.1158/0008-5472.CAN-08-4295

and CDK6, is inactivated either through deletion, mutation, or silencing in ~90% of T-ALL patient samples (14–17). Evidence that cyclin D–dependent kinase signaling is essential in NOTCH-driven T-ALL comes from analysis of the cyclin D3 knockout mouse. Expression of NOTCH1 NICD in wild-type bone marrow cells gives rise to T-ALL in recipient mice with 100% penetrance, whereas no leukemia develops when NICD is expressed in cyclin $D3^{-/-}$ bone marrow cells (18).

This study shows that baseline NOTCH pathway activity measured using a NOTCH target gene signature is predictive of sensitivity to a GSI, and hence, may provide a tool for patient stratification to enrich for response. Second, investigation of the molecular mechanisms of GSI response in T-ALL cells revealed that inhibition of NOTCH signaling induces the expression of CDK inhibitors, CDKN2D ($p19^{INK4d}$) and CDKN1B ($p27^{Kip1}$), thereby engaging RB-mediated arrest, and importantly, leading to cell cycle exit. Consistent with this mechanism of action, combined treatment of T-ALL cells with GSI and a small molecule inhibitor of CDK4 sensitizes T-ALL cells to GSI action.

Materials and Methods

Compounds. MRK-003 (active GSI) and MRK-006 (275-fold less active enantiomer control) were previously described (19). Stocks in DMSO were used for dilutions (10 mmol/L) described in this study. DMSO stocks (2.5 mmol/L) were used for dilutions of the CDK4 inhibitor, a 6-substituted indolocarbazole, 2-bromo-12,13-dihydro-5H-indolo[2,3-a]pyrrolo[3,4-c] carbazole-5,7(6H)-dione (Calbiochem, Inc). Selectivity of this CDK4 inhibitor is as follows: IC_{50}s in enzymatic assays are 76 nmol/L, 520 nmol/L, and 2.1 μmol/L for CDK4/cyclin D1, CDK2/cyclin E, and CDK1/cyclin B, respectively.

Cell culture and cell viability. Human T-ALL cell lines were purchased from American Type Culture Collection or Deutsche Sammlung von Mikroorganismen und Zellkulturen. Cell lines were maintained in RPMI supplemented with 10% to 15% fetal bovine serum and 2 mmol/L of glutamine. For GI_{50} (growth inhibition as measured by an ATP-based viability assay) analyses, T-ALL cell lines were plated in 96-well plates at 5,000 cells/well, except for T-ALL-1 cells which were plated at 10,000 cells/well. Cells were re-fed and resuspended with compound and medium on day 4. Viability assays were performed using the CellTiter-Glo kit (Promega) 7 days after compound addition. For larger scale compound treatments, T-ALL cell lines were plated in T-150 flasks at 200,000 cells/mL and treated with 5 μmol/L of GSI (MRK-003). Washout studies were performed using 10 μmol/L of GSI. T-150 cultures were also re-fed on day 4. The CDK4 inhibitor was used at 500 nmol/L in combination studies. mRNA was isolated from cells following treatment with DMSO, 0.1 or 1 μmol/L of GSI (MRK-003) for 3 days and microarray gene expression analysis was conducted as previously described (20).

Western blot. Standard Western blotting procedures were used. Blots were scanned using a Gel Doc (Bio-Rad) and quantitated using Quantity One software (Bio-Rad). RB underphosphorylated signal was quantitated as a ratio to total RB after actin normalization. Antibodies used as follows: RB-underphosphorylated (BD Biosciences) RB-Total, CDKN1B (Cell Signaling Technologies), CDKN2D (Zymed Laboratories), NOTCH1-NICD (Cell Signaling Technologies), and beta-actin (Abcam, Inc.). For NICD Western blot detection, refer to ref. (20). Anti-mouse or anti-rabbit secondary antibodies conjugated to horseradish peroxidase (Amersham) were used for chemiluminescent detection.

Flow cytometry. DNA content analysis was performed using propidium iodide/RNase buffer (BD Biosciences) or Draq5. Briefly, 1×10^6 cells were harvested and fixed with 70% ethanol for 20 min on ice, washed and then resuspended in 500 μL of propidium iodide buffer for 15 min at room temperature followed by analysis on flow cytometer (FACSCalibur, BD Biosciences). Draq5 staining was performed by incubating 200,000 live cells with 10 μmol/L of Draq5 for 5 min followed by flow cytometric analysis (488 nm excitation). Mini-chromosome maintenance complex component 6 (MCM6) staining was performed by harvesting 3×10^5 cells, fixing in 2% paraformaldehyde (BD Biosciences) for 20 min on ice, followed by permeabilization using Intra-Cyte wash buffer (Orion BioSolutions) for 45 min. Cells were washed twice and stained with MCM6-FITC antibody (BD Biosciences) at 1:200 dilution for 1 h on ice.

RNA isolation and quantitative PCR analysis. T-ALL cell lines were treated with DMSO or MRK-003 (active GSI) for 48 h and then harvested. RNA was isolated using the RNeasy Mini Kit (Qiagen). cDNA was synthesized using the High Capacity Archive kit (Applied Biosystems). Quantitative PCR was performed on an ABI 7900 using the ΔΔCT protocol using their inventoried TaqMan probes/primers for human CDKN2D, CDKN1B, and glyceraldehyde-3-phosphate dehydrogenase (as internal control). Analysis was performed using the SDS 2.2.2 software (Applied Biosystems).

Expression profiling analysis. Global expression profiling of the T-ALL cell lines was performed on MRK-003 and DMSO treated cells as previously reported (20). Genes which correlated with GSI sensitivity, GI_{50}, were determined by the transcriptional response (treated versus DMSO at $\log_{10}$ scale) of 15 T-ALL cell lines treated with GSI (0.1 and 1 μmol/L) for 3 days. To establish a threshold for selecting the genes whose expression significantly anticorrelated with the GI_{50}, a Monte Carlo simulation was conducted. Based on 100 simulations, genes which showed a correlation coefficient lower than −0.4 were selected as genes significantly ($P < 0.05$) anticorrelated with GI_{50} among the GSI-treated cell lines.

These genes were subjected to Ingenuity Pathway Analysis (Ingenuity Systems)[6]. Microarray data have been deposited in the GEO database under accession number GSE8416.

Chromatin immunoprecipitation assay. KOPTK1 cells treated with DMSO or 5 μmol/L of GSI (MRK-003) for 24 h were used for chromatin immunoprecipitation (ChIP) assays (EZ-chip kit; Millipore). Cells (2×10^7) were cross-linked in 1% formaldehyde. Chromatin was sheared to an average DNA size of 500 bp, then incubated overnight with 5 μg of anti–c-Myc (N262; Santa Cruz Biotechnology) or rabbit IgG antibodies. Immunoprecipitated DNA was washed, de–cross-linked and purified, then used in TaqMan PCR (Applied Biosystems) and PCR (GC-Rich PCR system; Roche).

The primers used for PCR of BSII are 5′-CCCTCTAGGAGGTGCTAAG-TAAATATTT-3′ and 5′-ACTGAGCCAGCAGGAAAGGA-3′. The primers and probes used for TaqMan PCR are listed in Supplemental Table S1.

Analysis of combined drug effects. Drug synergy was determined by the combination index method (non–constant ratio) using the CalcuSyn software.[7] Using the data obtained from the growth inhibition assays (Fig. 5*C*), combination index values were generated over a range of fractional growth inhibition. A combination index of 1 indicates an additive effect, a combination index <1 indicates synergy, and a combination index >1 indicates antagonism.

Virus production and T-ALL cell line infection. HEK293T cells were transfected with either the empty vector (MigR1) or a vector encoding the intracellular form of NOTCH1 (MigR1 NICD) along with pKatAmpho and pCMV-VSV-G using LipofectAMINE PLUS (Invitrogen). Viral supernatants were removed 60 h later, filtered, and used to infect T-ALL-1 cells in the presence of polybrene. Infected cells were collected by flow sorting of GFP+ cells.

***NOTCH1* sequencing.** Status of exon 26, exon 27, and exon 34 of *NOTCH1* in the T-ALL cell lines is indicated as previously described (4).

Results

Identification of a NOTCH pathway gene signature that predicts sensitivity to GSI. In a subset of human T-ALL cell lines with activating mutations in *NOTCH1*, treatment with GSIs leads to cell cycle arrest and cell death (4, 19). We have previously shown

[6] http://www.ingenuity.com/
[7] http://www.biosoft.com/

Published OnlineFirst March 24, 2009; DOI: 10.1158/0008-5472.CAN-08-4295

Table 1. Sensitivity of T-ALL cell lines to GSI

Cell line	*NOTCH1* status	NICD*	GI_{50} (μmol/L)†
T-ALL-1	Wild-type	0	0.11
KOPTK1	Mutated	3	0.15
DND41	Mutated	2	0.25
HPB-ALL	Mutated	3	0.38
RPMI8402	Mutated	3	0.86
CEM	Mutated	2	3.2
PF382	Mutated	3	3.2
HSB2	Wild-type	1	3.7
BE-13	Mutated	3	6.8
SUP-T11	Wild-type	0	7.1
JURKAT	Wild-type	3	>10
LOUCY	Wild-type	0	>10
MOLT-4	Mutated	3	>10
MOLT-16	Wild-type	0	>10
SKW-3	Mutated	1	>10

*NICD levels are reported qualitatively based on Western blot signal: 0, none; 1, low; 2, medium; 3, high.
† GI_{50}s are based on growth inhibition as measured by a 7-d ATP-based viability assay.

that several T-ALL cell lines with detectable levels of NICD are resistant to GSI treatment, suggesting that other measures of GSI sensitivity are needed (20). We measured GSI sensitivity by determining GI_{50} values (growth inhibition as measured by an ATP-based viability assay) for 15 T-ALL cell lines, after exposure to GSI (MRK-003) for 7 days. A comparison of this data to *NOTCH1* mutation status (*t* test; $P = 0.19$) and NICD levels (*t* test, 0 versus 1–3; $P = 0.35$) shows that neither mutation status nor NICD protein levels effectively identify T-ALL cell lines sensitive to GSI (Table 1).

We used transcriptional profiling to determine if a gene signature could be identified that predicts sensitivity to GSI in T-ALL. The 15 T-ALL cell lines described in Table 1 were profiled

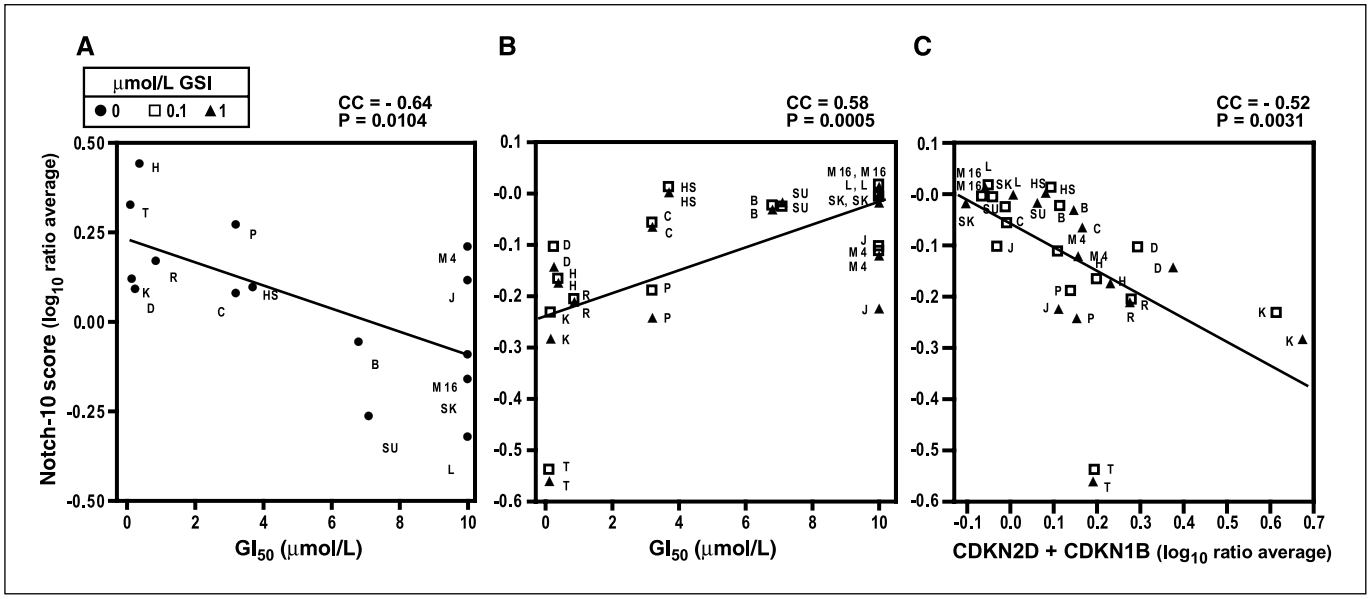

Figure 1. NOTCH pathway activity correlates with GSI sensitivity of T-ALL cell lines. *A,* cells with the highest NOTCH pathway activity were the most sensitive to GSI, MRK-003. NOTCH pathway activity was reported as the average mRNA expression of 10 NOTCH target genes (*HES-1, HES-4, HES-5, HEY-L, HEY-2, DTX1, c-MYC, NRARP, PTCRA*, and *SHQ1*), referred to as the "NOTCH-10 score" in 15 T-ALL cell lines. NOTCH pathway activity correlates with the growth inhibitory effect (GI_{50}) on these cell lines. BE-13 (*B*), CCRF-CEM (*C*), DND-41 (*D*), HPB-ALL (*H*), HSB-2 (*HS*), JURKAT (*J*), KOPTK-1 (*K*), LOUCY (*L*), MOLT-4 (*M4*), MOLT-16 (*M16*), PF-382 (*P*), RPMI-8402 (*R*), SKW-3 (*S*), SUPT-11 (*SU*), T-ALL-1 (*T*). *Top,* Pearson correlation coefficient (*CC*) and *P* values (*P*). *B,* GSI-induced changes in the NOTCH-10 score positively correlated with GSI sensitivity. GSI (0.1 or 1 μmol/L)-induced changes in mRNA expression for genes associated with the NOTCH-10 score (treated vs. DMSO) and shown as $\log_{10}$ ratio average were plotted against the GI_{50} for each cell line. *C,* GSI-induced decrease in Notch target gene expression was anticorrelated with induction of cell cycle genes CDKN2D (p19) and CDKN1B (p27). GSI (0.1 or 1 μmol/L)-induced changes in mRNA expression for genes associated with the NOTCH-10 score and averaged change in (CDKN2D-CDKN1B) expression were plotted as $\log_{10}$ ratio average (treated vs. DMSO) for each cell line.

Published OnlineFirst March 24, 2009; DOI: 10.1158/0008-5472.CAN-08-4295

and 10 NOTCH target genes (*HES-1, HES-4, HES-5, HEY-L, HEY-2, DTX1, C-MYC, NRARP, PTCRA*, and *SHQ1*; refs. 3, 9) were used to assess NOTCH pathway activity. A composite expression score for NOTCH pathway activity was determined by calculating the average expression value of 10 NOTCH target genes (*NOTCH-10*) for each of the 15 cell lines. This score was then compared with the GI_{50} of each cell line, which showed that the basal NOTCH pathway activity correlates with sensitivity to GSI (Fig. 1*A*). The presence of mutations in genes that modulate NOTCH signaling may explain why some resistant cell lines (JURKAT and MOLT-4) display a high signature score (see Discussion). Change in expression of the NOTCH-10 gene set in response to GSI treatment was also assessed. The 10-gene pathway signature was down-regulated in the GSI-sensitive cells, exhibiting a positive correlation to GSI sensitivity (Fig. 1*B*).

NOTCH inhibition by GSI and the induction of a G_1-S checkpoint gene set in T-ALL cells. In order to better understand the biological processes that are related to GSI efficacy downstream of NOTCH inhibition, we utilized Ingenuity Pathway Analysis to identify gene sets that were enriched in a manner which correlated with GSI sensitivity across the T-ALL cell line panel. Genes involved in the G_1-S checkpoint were found to be overrepresented among sensitivity-related, GSI-modulated genes (P = 0.0016). This is consistent with observations that GSI treatment leads to a slow accumulation of cells in the G_1-G_0 phase of the cell cycle (4, 9, 19). Among the G_1-S genes regulated by GSI were *CDKN2D* and *CDKN1B*, which act as inhibitors of the G_1-S transition by blocking the activity of the cyclin-dependent kinases CDK4, CDK6, and CDK2. The induction of *CDKN2D* and *CDKN1B* by GSI correlated with the change in NOTCH signaling across the cell line panel, as measured by the 10-gene NOTCH signature (Fig. 1*C*). The induction of these CDK inhibitors together or alone correlated with the sensitivity to NOTCH inhibition among the T-ALL cell line panel (*CDKN1B* correlation coefficient = −0.677, P = 0.0056; *CDKN2D* correlation coefficient = −0.529, P = 0.035; Fig. 2*A*). Quantitative reverse transcription-PCR analysis of T-ALL-1, DND-41, and RPMI-8402 cells treated for 48 hours with GSI compared with DMSO control showed between a 2.5-fold and

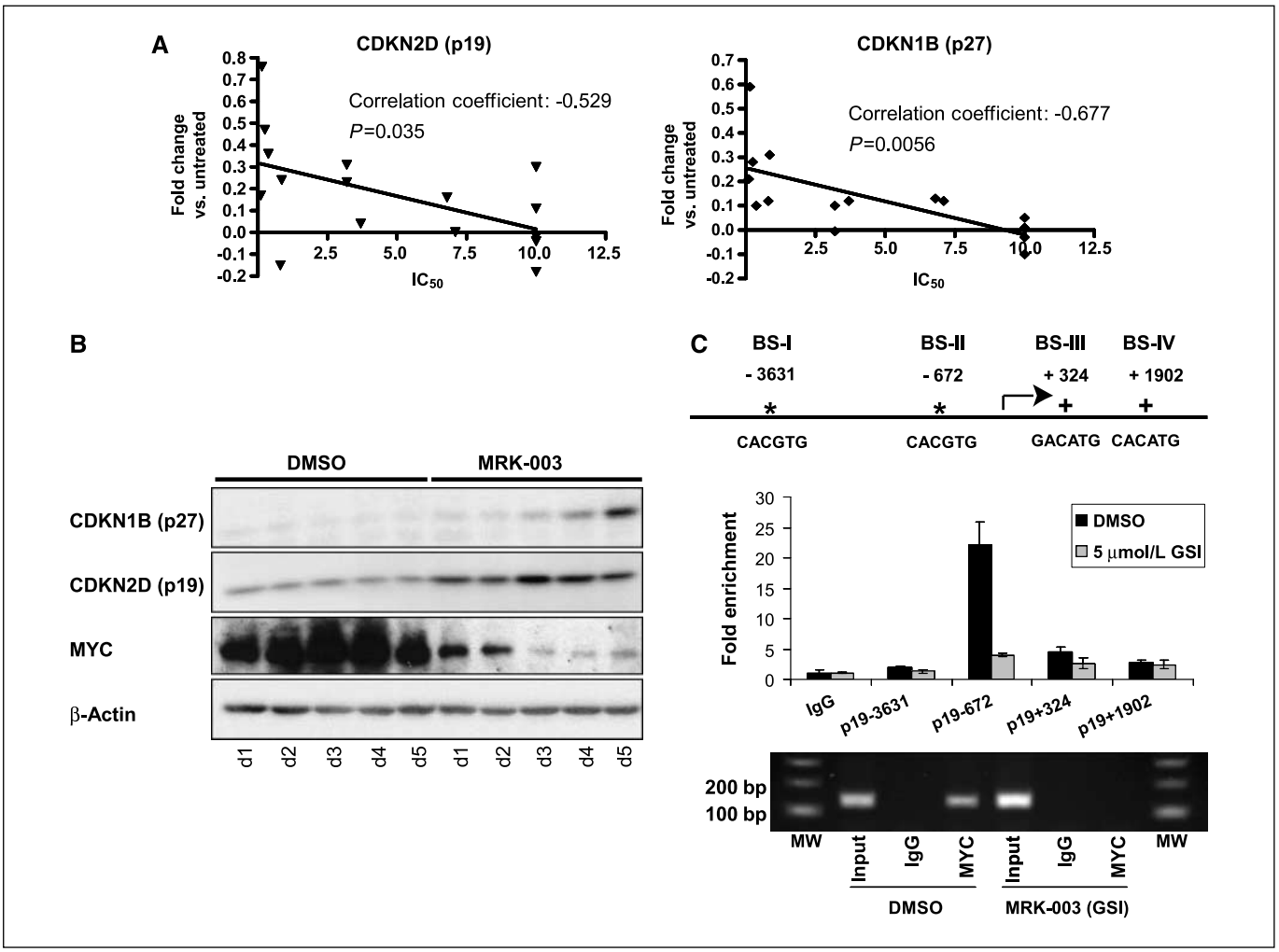

Figure 2. GSI-induced up-regulation of CDKN2D and CDKN1B. *A,* GSI sensitivity of the T-ALL cell lines correlates with the induction of CDKN2D (*left*) and CDKN1B (*right*) after exposure to GSI. *B,* Western blot analysis of CDKN2D, CDKN1B, and MYC protein expression in T-ALL-1 cells over 5 d of treatment with 1 μmol/L of GSI (*MRK-003*). *C,* ChIP assay showing GSI-modulated binding of MYC to *CDKN2D. Top,* schematic of *CDKN2D* 5′ regulatory region. *Arrow,* the transcriptional starting site. The canonical (*) and noncanonical (+) E boxes. *Middle,* quantification of MYC binding to each putative site by TaqMan PCR analysis (presented as fold enrichment relative to IgG). ChIP was performed on KOPTK1 cells treated with DMSO and 5 μmol/L of MRK-003 (*GSI*) for 24 h using anti-MYC antibody or normal IgG as a control. *Bottom,* the specificity of MYC binding to BS-II was confirmed by PCR.

Published OnlineFirst March 24, 2009; DOI: 10.1158/0008-5472.CAN-08-4295

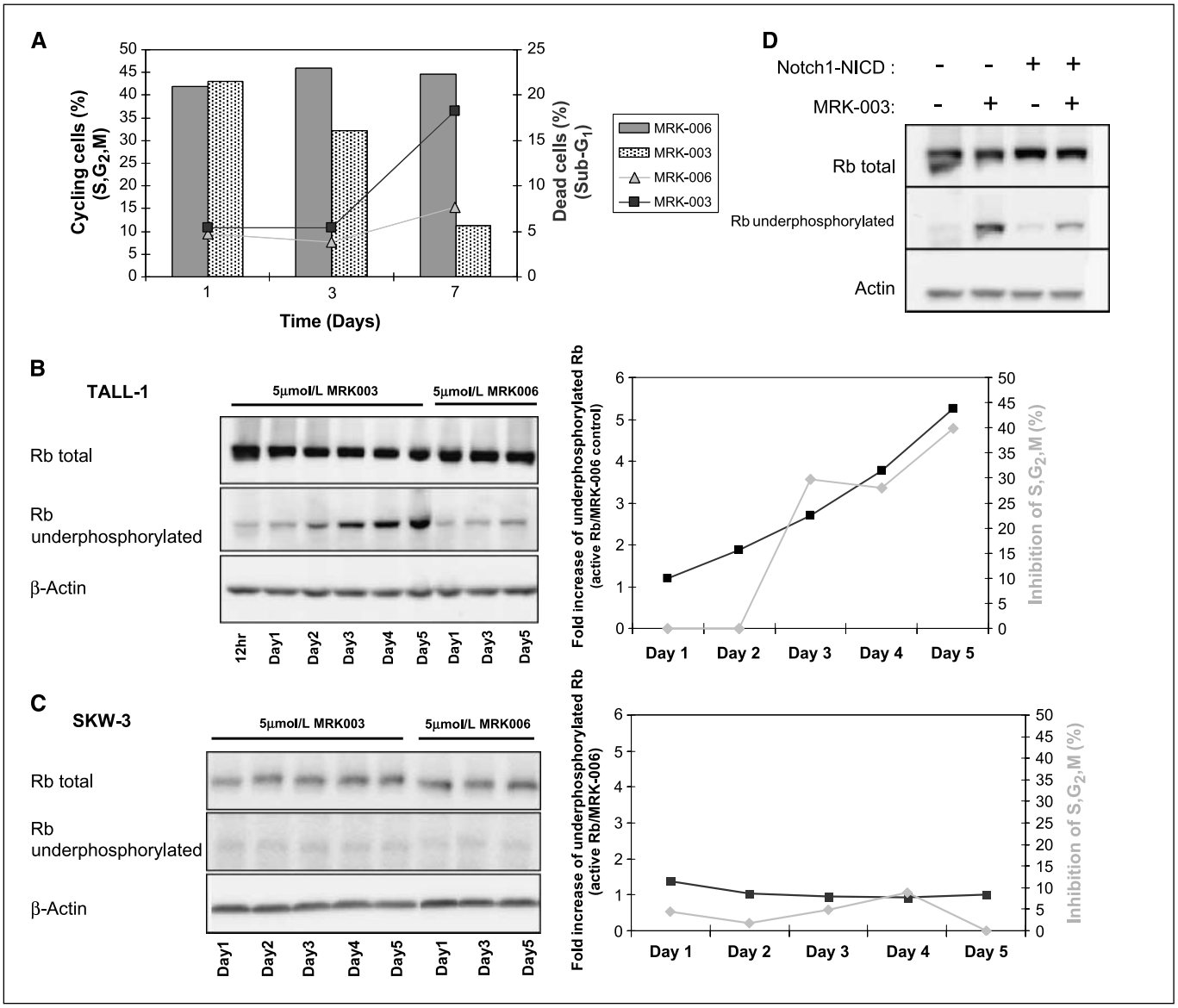

Figure 3. GSI inhibits RB phosphorylation in T-ALL-1 but not SKW3 cells. *A,* kinetics of cell cycle arrest (*bar graph:* S, G_2-M population) and death (*line graph:* sub-G_1 population) in T-ALL-1 cells after GSI (MRK-003, 5 μmol/L) or enantiomer control (MRK-006, 5 μmol/L) treatment for 1, 3, or 7 d. Quantitations based on flow cytometric data. *B,* Western blot analysis of RB underphosphorylated species (active form of RB) on each of 5 d of GSI vs. control treatment in T-ALL-1 cells. *Graph,* kinetic comparison of inhibition of RB phosphorylation (ratio of RB underphosphorylated—MRK-003/MRK-006) to percentage of cell cycle inhibition [100% − (S, G_2-M for MRK-003/MRK-006)]. *C,* similar analysis as in *B* for a GSI-insensitive cell line, SKW3. *D,* Western blot was performed to assess level of rescue of the inhibition of RB phosphorylation in T-ALL-1 cells constitutively expressing NICD vs. vector control after 3 d GSI (MRK-003, 1 μmol/L) treatment. NICD constitutive expression in T-ALL-1 cells reduces GSI inhibition of RB phosphorylation.

3.5-fold up-regulation of *CDKN2D* and between a 1.3-fold and 2.8-fold up-regulation of *CDKN1B* (Supplementary Fig. S1).

Western blot kinetic analysis confirmed that CDKN2D was induced 3-fold at the protein level within 24 hours of exposure to the active MRK-003 but not by the DMSO control (Fig. 2*B*). Importantly, CDKN2D up-regulation was observed prior to the onset of the earliest stage of cell cycle arrest. *MYC* is a direct target gene of NOTCH1 and effector of NOTCH signaling (9, 11, 21). A previous study suggested that the *CDKN2D* gene is bound and repressed by MYC (22), providing a possible mechanism by which GSI-mediated inhibition of NOTCH results in the induction of *CDKN2D*. Treatment of T-ALL cells with GSI leads to a reduction of MYC protein and a 4-fold decrease in the occupancy of a MYC binding site 672 bp upstream of the *CDKN2D* transcriptional start site, as measured by ChIP/reverse transcription-PCR analysis (Fig. 2*B* and *C*). CDKN1B protein was induced 1.5-fold by day 3, reaching 6-fold by day 5 of GSI treatment (Fig. 2*B*). This is consistent with data indicating that CDKN1B is regulated by NOTCH via transcriptional and posttranslational mechanisms (23–26).

GSI inhibits RB phosphorylation prior to cell cycle arrest. Treatment of T-ALL-1 cells with MRK-003 led to a reduction in the percentage of actively cycling cells (Fig. 3*A*). This effect became detectable after 72 hours of treatment. An enantiomer of MRK-003, MRK-006, that lacks GSI activity had no such effect on the cell cycle.

Published OnlineFirst March 24, 2009; DOI: 10.1158/0008-5472.CAN-08-4295

We find that GSI treatment resulted in the elevation of the active hypophosphorylated form of RB, following the induction of the CDKN2D (Fig. 3*B*). The active, hypophosphorylated form of RB was detected within the first 2 days of GSI exposure in T-ALL cells and increased steadily to day 5, whereas the inhibition of the cell cycle was detectable by day 3 (Fig. 3*B*). The inactive enantiomer, MRK-006, did not affect RB phosphorylation or cell cycle progression and GSI-insensitive SKW-3 cells showed no significant increase in the active RB species (Fig. 3*C*). Expression of NOTCH1 NICD in T-ALL-1 cells abrogated the inhibition of RB phosphorylation caused by GSI (Fig. 3*D*). These results suggest that the cell cycle arrest caused by inhibition of the NOTCH signaling pathway in T-ALL cells is mediated by derepression of RB activity. Following the onset of cell cycle arrest, after 3 days of GSI treatment, a sub-G_1 cell population became detectable, indicative of cell death (Fig. 3*A*).

Continuous GSI exposure is unnecessary to induce phenotypic effects. DNA content alone cannot distinguish cells that are arrested in G_1 from cells that have exited the cell cycle (G_0). In order to distinguish between these two possibilities, cells were stained with a fluorescently conjugated antibody to MCM6. MCM6, a core component of the DNA replication preinitiation complex, is expressed during all phases of the cell cycle but is undetectable when cells have exited the cell cycle (27, 28). We assessed MCM6 protein expression in T-ALL-1 cells by flow cytometry after 5 days of GSI treatment (Fig. 4*A*; Supplementary Fig. S2). Down-regulation of MCM6 was observed as compared with untreated and MRK-006 controls. In control samples (treated with inactive MRK-006), 97% of cells with 2N DNA content express high levels of MCM6 protein, whereas this percentage dropped to only 4% in samples treated with MRK-003 (Supplementary Fig. S2). Gene expression profiling

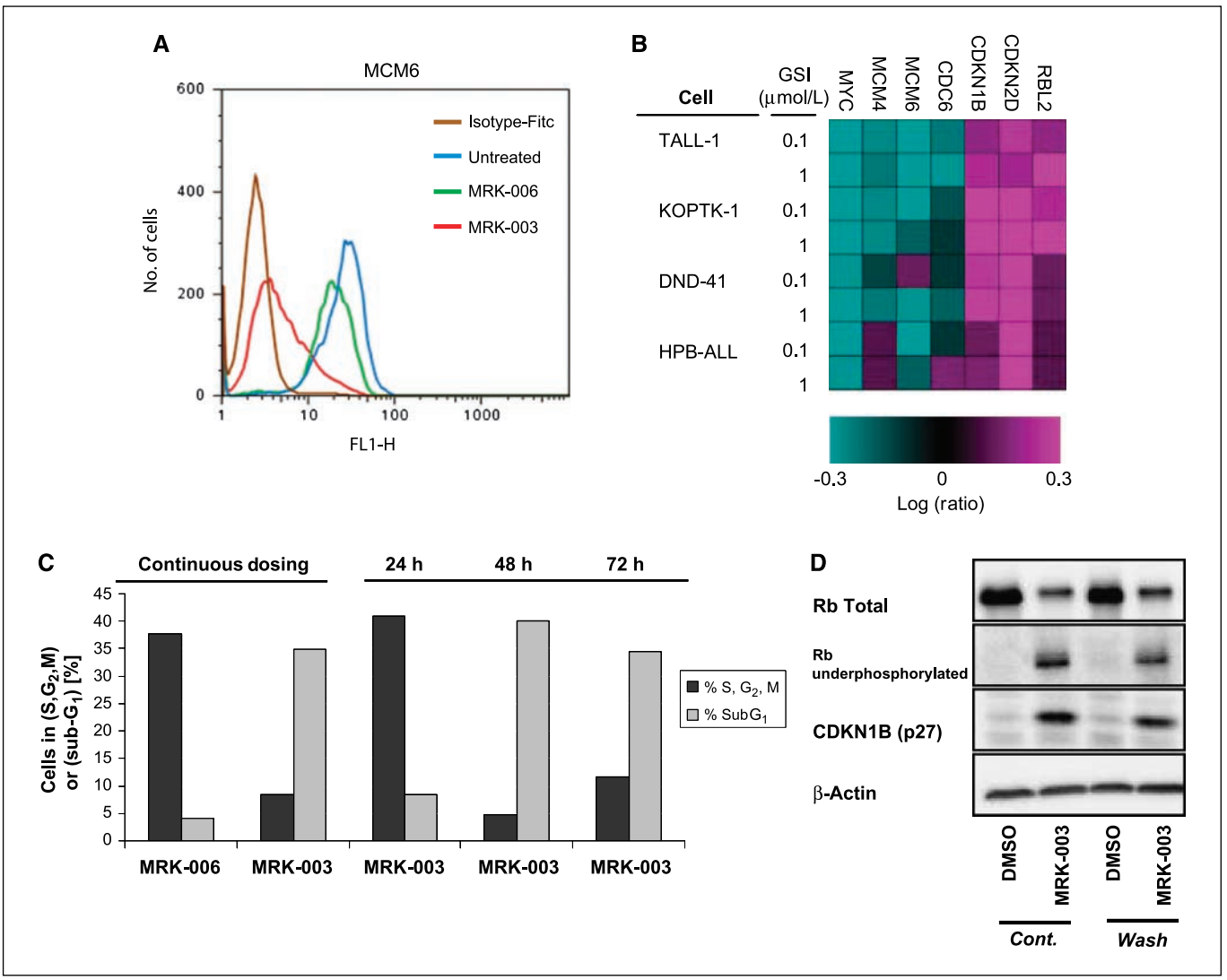

Figure 4. GSI induces cell cycle exit and continuous exposure is not required. *A,* flow cytometric analysis of MCM6 staining in T-ALL-1 cells on day 5 after treatment with 1 μmol/L of GSI (MRK-003), 1 μmol/L of MRK-006, and untreated controls. A FITC-conjugated isotype control was used to assess background fluorescence. Down-regulation of MCM6 is associated with cell cycle exit. *B,* a heat-map of mRNA levels of key cell cycle genes known to be involved in cell cycle exit, after exposure to 1 μmol/L or 100 nmol/L of MRK-003 (*GSI*) for 72 h in four sensitive T-ALL cell lines. Similar to MYC, multiple components of the DNA synthesis preinitiation complex (*MCM4, MCM6*, and *CDC6*) are repressed, whereas CDKN2D, CDKN1B and RBL2 are induced. *C,* quantitation of S,G_2-M (cycling) and sub-G_1 (dead) populations of DNA content analysis (Supplementary Fig. S1). Draq5 was used in T-ALL-1 cells on day 8 after continuous exposure with 10 μmol/L of GSI (MRK-003) or 10 μmol/L of MRK-006 control as compared with 24, 48, or 72 h exposure to GSI and then compound washout. *D,* Western blot analysis of total RB, RB underphosphorylated, and CDKN1B (p27) after continuous dosing with 10 μmol/L of MRK-003 (GSI; *Cont.*) or 48 h treatment with 10 μmol/L of MRK-003 (GSI) followed by compound washout (*Wash*) in T-ALL-1 cells. Cells were harvested for Western blot analysis on day 8 of treatment.

Published OnlineFirst March 24, 2009; DOI: 10.1158/0008-5472.CAN-08-4295

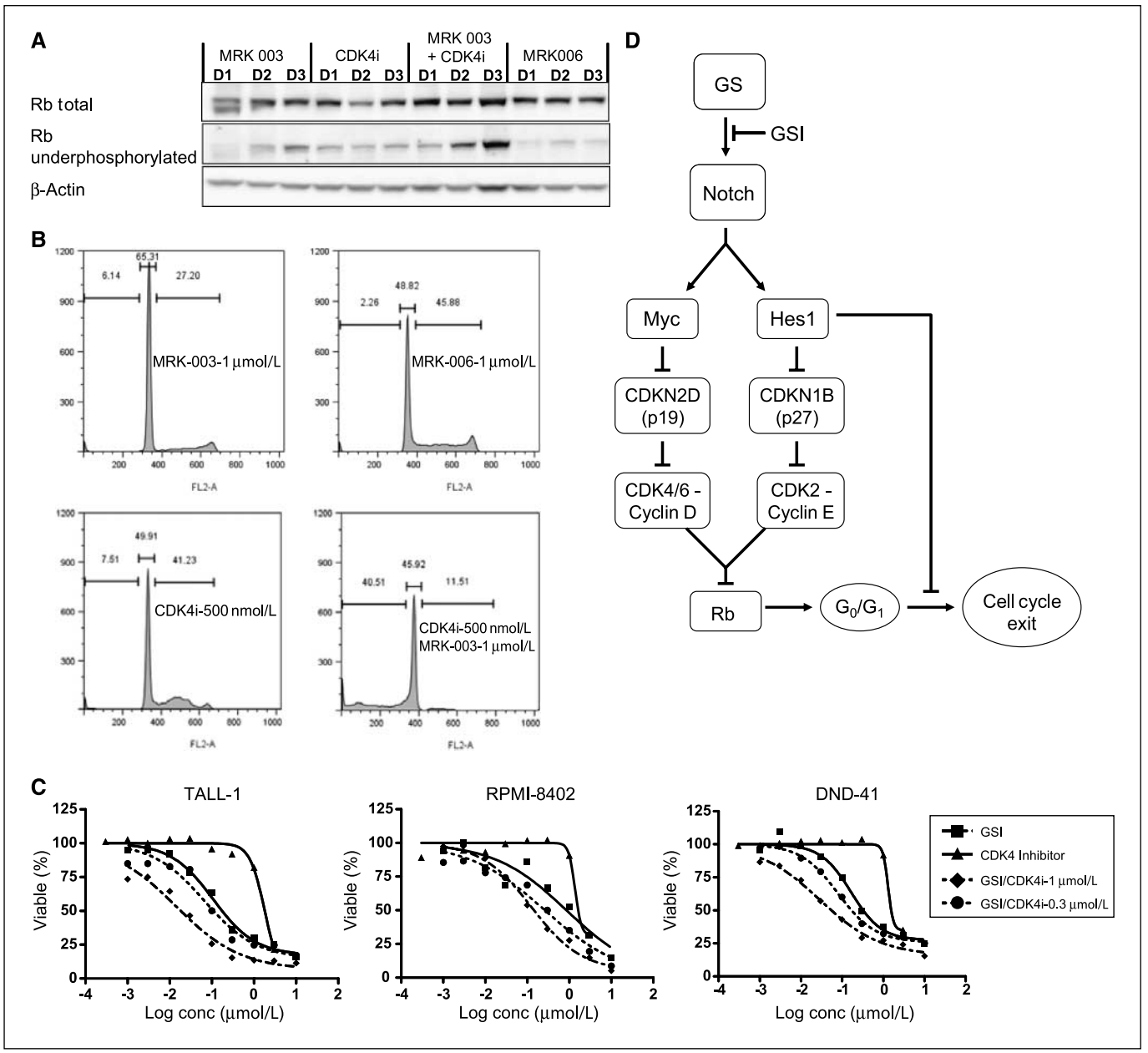

Figure 5. GSI in combination with a CDK4 inhibitor potently enhances cell cycle arrest and death in T-ALL-1 cells. *A,* Western blot analysis of induction of active RB (*underphosphorylated*) after treatments with either GSI (MRK-003, 1 μmol/L), CDK4 inhibitor (Calbiochem, 500 nmol/L), MRK-006 control (1 μmol/L), or combination of GSI + CDK4 inhibitor. *B,* DNA content analysis of conditions described in *A. C,* sensitization of T-ALL cell lines to GSI with a CDK4 inhibitor. GI_{50} curve analysis of three GSI-sensitive cell lines (T-ALL-1, DND-41, RPMI-8402) to GSI treatment alone compared with combination treatment with GSI and a CDK4 inhibitor in a 7-d ATP viability assay. *D,* a model of GSI-induced cell cycle effects in T-ALL cells, involving the engagement of the RB pathway and the role of HES1 inhibition leading to exit from the cell cycle.

data shows multiple components of the DNA synthesis preinitiation complex (MCM4, MCM6, and CDC6) are also repressed in GSI-sensitive T-ALL cell lines (Fig. 4*B*). Further evidence that MRK-003 induces cell cycle withdrawal is provided by high CDKN1B levels observed by day 5 of treatment (Figs. 2*B* and 4*D*; ref. 23). Additionally, the pocket protein family member, RBL2/p130, has also been shown to increase when cells exit the cell cycle into the G_0 quiescent state (Fig. 4*B*; refs. 29–31). We hypothesized that if GSI treatment of T-ALL-1 cells results in cell cycle exit, then continuous treatment with GSI may not be required. We compared the cell cycle profiles of cells after continuous GSI treatment for 8 days with those treated for 24, 48, or 72 hours, followed by compound removal with response measured on day 8. Interestingly, 48 hours of GSI treatment was sufficient to induce cell cycle arrest (7.5-fold reduction in the S, G_2-M cell population) and cell death (10.5-fold increase in the sub-G_1 population) similar to continuous treatment for 8 days (Fig. 4*C*; Supplementary Fig. S3). Furthermore, sustained inhibition of RB phosphorylation and up-regulation of CDKN1B are observed 6 days after compound removal (Fig. 4*D*), suggesting these cells have truly exited from the cell cycle. Similar effects of pulsetile treatment (48-hour washout) on cell cycle arrest was observed using DND-41 cells (Supplementary Fig. S4*A*). NICD,

Published OnlineFirst March 24, 2009; DOI: 10.1158/0008-5472.CAN-08-4295

which could be measured in DND-41 but not T-ALL-1 cells, recovers within 48 hours following compound washout (Supplementary Fig. S4*B*). Therefore, sustained inhibition of the S, G_2-M population and persistent induction of CDKN1B are observed despite rapid recovery of NICD levels (Supplementary Fig. S4*A* and *C*). These results show that 48-hour exposure to GSI is equally effective as continuous treatment, over an 8-day period, and provides additional support for GSI-mediated cell cycle exit in NOTCH pathway–dependent T-ALL cells.

Combination of GSI with a CDK4 inhibitor results in potent cell cycle arrest and death. The induction of CDKN2D and inhibition of CDK-mediated RB-phosphorylation by GSI suggested that treatment with a synthetic CDK4 inhibitor could sensitize T-ALL cells to GSI. Therefore, T-ALL-1 cells were treated with a combination of MRK-003 and cyclin D1-CDK4 inhibitor (6-substituted indolocarbazole) and assessed for effects on RB phosphorylation, cell cycle arrest, and cell viability. We observed a more potent induction of hypophosphorylated RB within the first 3 days of treatment as compared with GSI or CDK4 inhibitor treatment alone (Fig. 5*A*). DNA content analysis showed a 3-fold reduction in the S, G_2-M populations and a 4-fold up-regulation of the nonviable sub-G_1 population by day 5 of combination treatment as compared with GSI alone (Fig. 5*B*). GSI effects on cell viability were enhanced considerably by combination treatment, reducing GI_{50} values by 6-fold to 8-fold in three different GSI-sensitive T-ALL cell lines (Fig. 5*C*; Supplementary Table S2). Synergistic growth inhibition was observed in these cell lines at multiple drug concentrations, yielding combination index values of <1 (Supplementary Fig. S5*A*–*C*). The CDK4 inhibitor did not enhance GSI effects in GSI-insensitive T-ALL cells, consistent with a lack of NOTCH pathway dependence in these lines. These results indicate that a combination treatment of GSI and a CDK4 inhibitor potently enhance and accelerate cell cycle arrest and death in NOTCH-dependent T-ALL cell lines. They further strengthen the role of the RB pathway in the GSI response and suggest a possible combination therapy for cancer patients with activated NOTCH signaling.

Discussion

Understanding the mechanism of GSI-induced cell death and the ability to accurately identify patients most likely to respond to GSI is critical to the successful clinical development of this novel therapy. It is apparent from the treatment of T-ALL cell lines with GSIs that the presence of an activating mutation in *NOTCH1* or constitutive expression of NICD does not effectively predict response. We find that a gene signature composed of 10 NOTCH target genes is an effective reporter of pathway activity and that this metric correlates with cellular sensitivity to GSI. Hence, this signature may be useful as a patient stratification tool for T-ALL as well as other NOTCH-activated tumor types being considered for GSI therapy or other therapeutics that target the NOTCH pathway. Although levels of NOTCH target genes will aid in the identification of patients more likely to respond to GSI, additional mechanisms of resistance may exist. Such mechanisms seem to be present in two cell lines, JURKAT and MOLT-4, which display elevated NOTCH target gene expression and whose expression is modulated by GSI, however, remain insensitive to treatment. Both of these cell lines are deficient in the expression of PTEN (data not shown; ref. 32). In addition, JURKAT cells express a mutated form of FBW7 (20). The mutation of both PTEN and FBW7 are known to confer resistance to GSI (20, 33, 34).

Previous studies have linked activated NOTCH signaling to aberrant cell cycle progression and show that GSIs induce cell cycle arrest in a subset of T-ALL cell lines. This study shows the molecular events leading to growth arrest upon GSI treatment in GSI-sensitive T-ALL cell lines. We show that prior to the onset of cell cycle arrest, GSI induces *CDKN2D*, which coincides with the inhibition of MYC. Genomic analysis of MYC binding and gene regulation indicated that MYC functions as a transcriptional repressor of *CDKN2D* (22), which is supported by our findings that MYC binds to the *CDKN2D* promoter in T-ALL cells in a GSI-sensitive manner. GSI treatment also led to the induction of CDKN1B as previously observed (24).

The inductions of CDKN2D and CDKN1B (inhibitors of CDK4/6 and CDK2, respectively) are associated with the inhibition of RB phosphorylation, and hence, RB activation. Previous genetic studies indicate that deregulation of RB-mediated cell cycle control through loss of the CDK inhibitor gene CDKN2A (p16) is a critical, if not essential mechanism, during T-ALL leukemogenesis (35). Moreover, deletion of cyclin D3, which promotes CDK4 and CDK6 activity, prevents the development of leukemia in the context of activated NOTCH1 in mice (18). We propose that GSI-induced expression of CDKN2D and CDKN1B restores RB-mediated growth control in T-ALL cells that depend on deregulated cyclin D–dependent kinase activity.

Critical decisions regarding growth versus quiescence are made in the G_1 phase of the cell cycle, which is governed by the phosphorylation state of RB (36). Although CDKN2D induction occurs prior to the onset of cell cycle arrest, the elevation of CDKN1B occurs later. Hence, CDKN1B may not be a primary event in driving the initial accumulation in G_1-G_0, but may play an important role in the transition to a durable cell cycle exit in cooperation with CDKN2D (37). Hypophosphorylated RB as well as other RB family members, RBL1/p107 and RBL2/p130, are necessary to efficiently halt the proliferation of cells to facilitate their exit from cell cycle into G_0 and promote differentiation (29, 30). The RB family proteins have unique and overlapping functions in tumorigenesis, and both RBL1/p107 and RBL2/p130 can compensate for RB inactivation or loss (30). We show that in addition to the G_1 cell cycle arrest previously reported, T-ALL cells exit the cell cycle upon GSI treatment. Consequently, short-term exposure with GSI (48 hours) is sufficient to induce similar phenotypic effects as continuous exposure, indicating that a finite period of NOTCH inhibition can lead to a long-term, apparently irreversible, state change characterized by cell cycle exit. This has important clinical implications as it suggests that intermittent dosing may be sufficient to provide antitumor activity, and would be expected to alleviate toxicities associated with continuous exposure to GSI.

Based on the data presented here and in other recent reports, we propose a model by which GSI inhibition of NOTCH signaling in T-ALL cells leads to arrest in G_1 followed by cell cycle exit (Fig. 5*D*). NOTCH inhibition simultaneously represses MYC and HES1 expression. Blockade of MYC expression leads to derepression of CDKN2D whereas HES1 inhibition leads to the induction of CDKN1B (25), resulting in combined inhibition CDK4/6 and CDK2, elevated levels of hypophosphorylated, active RB, and G1 arrest. A recent report has shown that HES1 is required to prevent irreversible cell cycle exit of quiescent cells (38). Hence, we suggest that GSI inhibition of HES1 has an additional role in allowing G_1-arrested cells to exit the cell cycle.

Finally, we show that a small molecule CDK4 inhibitor sensitizes T-ALL cells to GSI. This underscores that the CDK4/6-RB pathway is

an important downstream mechanism through which GSI inhibits the proliferation of T-ALL cells. These results suggest a rational combination strategy to increase the therapeutic response to GSI in treating T-ALL and other cancers with activated NOTCH signaling.

Disclosure of Potential Conflicts of Interest

A.T. Look: research support SRA and honoraria from speakers bureau, from Merck, and patents on Notch mutations and signature filed. All authors, except J. O'Neil and A.T. Look, are or were employed by Merck & Co., Inc., which is developing GSI.

Acknowledgments

Received 11/10/08; revised 1/14/09; accepted 1/22/09; published OnlineFirst 3/24/09.

Grant support: Merck Research Laboratories (A.T. Look) and a Harvard Medical School Hematology Training Grant (J. O'Neil).

The costs of publication of this article were defrayed in part by the payment of page charges. This article must therefore be hereby marked *advertisement* in accordance with 18 U.S.C. Section 1734 solely to indicate this fact.

We acknowledge the Rosetta GELS group for microarray profiling and Jon Aster for MigR1 and MigR1 NICD vectors; we also thank Jennifer Tammam, Clay Efferson, Takaomi Sanda, Pradip Majumder, and Raphael Kopan for their guidance and support; and Lynn Winter for assistance with graphics.

References

1. Artavanis-Tsakonas S, Rand MD, Lake RJ. Notch signaling: cell fate control and signal integration in development. Science 1999;284:770–6.
2. Mumm JS, Kopan R. Notch signaling: from the outside in. Dev Biol 2000;228:151–65.
3. Grabher C, von Boehmer H, Look AT. Notch 1 activation in the molecular pathogenesis of T-cell acute lymphoblastic leukaemia. Nat Rev Cancer 2006;6:347–59.
4. Weng AP, Ferrando AA, Lee W, et al. Activating mutations of NOTCH1 in human T cell acute lymphoblastic leukemia. Science 2004;306:269–71.
5. Zhu YM, Zhao WL, Fu JF, et al. NOTCH1 mutations in T-cell acute lymphoblastic leukemia: prognostic significance and implication in multifactorial leukemogenesis. Clin Cancer Res 2006;12:3043–9.
6. Ellisen LW, Bird J, West DC, et al. TAN-1, the human homolog of the Drosophila notch gene, is broken by chromosomal translocations in T lymphoblastic neoplasms. Cell 1991;66:649–61.
7. Reynolds TC, Smith SD, Sklar J. Analysis of DNA surrounding the breakpoints of chromosomal translocations involving the beta T cell receptor gene in human lymphoblastic neoplasms. Cell 1987;50:107–17.
8. Pear WS, Aster JC, Scott ML, et al. Exclusive development of T cell neoplasms in mice transplanted with bone marrow expressing activated Notch alleles. J Exp Med 1996;183:2283–91.
9. Palomero T, Lim WK, Odom DT, et al. NOTCH1 directly regulates c-MYC and activates a feed-forward-loop transcriptional network promoting leukemic cell growth. Proc Natl Acad Sci U S A 2006;103:18261–6.
10. Sharma VM, Calvo JA, Draheim KM, et al. Notch1 contributes to mouse T-cell leukemia by directly inducing the expression of c-myc. Mol Cell Biol 2006;26:8022–31.
11. Weng AP, Millholland JM, Yashiro-Ohtani Y, et al. c-Myc is an important direct target of Notch1 in T-cell acute lymphoblastic leukemia/lymphoma. Genes Dev 2006;20:2096–109.
12. Chan SM, Weng AP, Tibshirani R, Aster JC, Utz PJ. Notch signals positively regulate activity of the mTOR pathway in T-cell acute lymphoblastic leukemia. Blood 2007;110:278–86.
13. Vilimas T, Mascarenhas J, Palomero T, et al. Targeting the NF-κB signaling pathway in Notch1-induced T-cell leukemia. Nat Med 2007;13:70–7.
14. Cayuela JM, Hebert J, Sigaux F. Homozygous MTS1 (p16INK4A) deletion in primary tumor cells of 163 leukemic patients. Blood 1995;85:854.
15. Hebert J, Cayuela JM, Berkeley J, Sigaux F. Candidate tumor-suppressor genes MTS1 (p16INK4A) and MTS2 (p15INK4B) display frequent homozygous deletions in primary cells from T- but not from B-cell lineage acute lymphoblastic leukemias. Blood 1994;84:4038–44.
16. Iravani M, Dhat R, Price CM. Methylation of the multi tumor suppressor gene-2 (MTS2, CDKN1, p15INK4B) in childhood acute lymphoblastic leukemia. Oncogene 1997;15:2609–14.
17. Ohnishi H, Kawamura M, Ida K, et al. Homozygous deletions of p16/MTS1 gene are frequent but mutations are infrequent in childhood T-cell acute lymphoblastic leukemia. Blood 1995;86:1269–75.
18. Sicinska E, Aifantis I, Le Cam L, et al. Requirement for cyclin D3 in lymphocyte development and T cell leukemias. Cancer Cell 2003;4:451–61.
19. Lewis HD, Leveridge M, Strack PR, et al. Apoptosis in T cell acute lymphoblastic leukemia cells after cell cycle arrest induced by pharmacological inhibition of notch signaling. Chem Biol 2007;14:209–19.
20. O'Neil J, Grim J, Strack P, et al. FBW7 mutations in leukemic cells mediate NOTCH pathway activation and resistance to gamma-secretase inhibitors. J Exp Med 2007;204:1813–24.
21. Sharma VM, Draheim KM, Kelliher MA. The Notch1/c-Myc pathway in T cell leukemia. Cell Cycle 2007;6:927–30.
22. Zeller KI, Zhao X, Lee CW, et al. Global mapping of c-Myc binding sites and target gene networks in human B cells. Proc Natl Acad Sci U S A 2006;103:17834–9.
23. Bashir T, Dorrello NV, Amador V, Guardavaccaro D, Pagano M. Control of the SCF(Skp2-1) ubiquitin ligase by the APC/C(Cdh1) ubiquitin ligase. Nature 2004;428:190–3.
24. Dohda T, Maljukova A, Liu L, et al. Notch signaling induces SKP2 expression and promotes reduction of p27Kip1 in T-cell acute lymphoblastic leukemia cell lines. Exp Cell Res 2007;313:3141–52.
25. Murata K, Hattori M, Hirai N, et al. Hes1 directly controls cell proliferation through the transcriptional repression of p27Kip1. Mol Cell Biol 2005;25:4262–71.
26. Sarmento LM, Huang H, Limon A, et al. Notch1 modulates timing of G1-S progression by inducing SKP2 transcription and p27 Kip1 degradation. J Exp Med 2005;202:157–68.
27. Leone G, DeGregori J, Yan Z, et al. E2F3 activity is regulated during the cell cycle and is required for the induction of S phase. Genes Dev 1998;12:2120–30.
28. Schrader C, Janssen D, Klapper W, et al. Minichromosome maintenance protein 6, a proliferation marker superior to Ki-67 and independent predictor of survival in patients with mantle cell lymphoma. Br J Cancer 2005;93:939–45.
29. Sun A, Bagella L, Tutton S, Romano G, Giordano A. From G0 to S phase: a view of the roles played by the retinoblastoma (Rb) family members in the Rb-E2F pathway. J Cell Biochem 2007;102:1400–4.
30. Wikenheiser-Brokamp KA. Retinoblastoma family proteins: insights gained through genetic manipulation of mice. Cell Mol Life Sci 2006;63:767–80.
31. Xue Jun H, Gemma A, Hosoya Y, et al. Reduced transcription of the RB2/p130 gene in human lung cancer. Mol Carcinog 2003;38:124–9.
32. Shan X, Czar MJ, Bunnell SC, et al. Deficiency of PTEN in Jurkat T cells causes constitutive localization of Itk to the plasma membrane and hyperresponsiveness to CD3 stimulation. Mol Cell Biol 2000;20:6945–57.
33. Palomero T, Sulis ML, Cortina M, et al. Mutational loss of PTEN induces resistance to NOTCH1 inhibition in T-cell leukemia. Nat Med 2007;13:1203–10.
34. Thompson BJ, Buonamici S, Sulis ML, et al. The SCFFBW7 ubiquitin ligase complex as a tumor suppressor in T cell leukemia. J Exp Med 2007;204:1825–35.
35. Fasseu M, Aplan PD, Chopin M, et al. p16INK4A tumor suppressor gene expression and CD3epsilon deficiency but not pre-TCR deficiency inhibit TAL1-linked T-lineage leukemogenesis. Blood 2007;110:2610–9.
36. Massague J. G1 cell-cycle control and cancer. Nature 2004;432:298–306.
37. Cunningham JJ, Levine EM, Zindy F, Goloubeva O, Roussel MF, Smeyne RJ. The cyclin-dependent kinase inhibitors p19(Ink4d) and p27(Kip1) are coexpressed in select retinal cells and act cooperatively to control cell cycle exit. Mol Cell Neurosci 2002;19:359–74.
38. Sang L, Coller HA, Roberts JM. Control of the reversibility of cellular quiescence by the transcriptional repressor HES1. Science 2008;321:1095–100.

Cancer Research
The Journal of Cancer Research (1916–1930) | The American Journal of Cancer (1931–1940)

AACR American Association for Cancer Research

Inhibition of NOTCH Signaling by Gamma Secretase Inhibitor Engages the RB Pathway and Elicits Cell Cycle Exit in T-Cell Acute Lymphoblastic Leukemia Cells

Sudhir S. Rao, Jennifer O'Neil, Cole D. Liberator, et al.

Cancer Res 2009;69:3060-3068. Published OnlineFirst March 24, 2009.